

First evidence for states in Hg nuclei with deformations between normal and super deformation

W. C. Ma, J. H. Hamilton, A. V. Ramayya, L. Chaturvedi, J. K. Deng, W. B. Gao,
Y. R. Jiang, J. Kormicki, and X. W. Zhao

Physics Department, Vanderbilt University, Nashville, Tennessee 37235

N. R. Johnson, J. D. Garrett, I. Y. Lee, C. Baktash, and F. K. McGowan
Oak Ridge National Laboratory, Oak Ridge, Tennessee 37831

W. Nazarewicz* and R. Wyss

Joint Institute for Heavy Ion Research, Oak Ridge, Tennessee 37831

(Received 30 March 1992)

High-spin states in ^{186}Hg with a quadrupole deformation of $\beta_2=0.34(4)$ have been established from measured gamma-ray coincidences and lifetimes. These data, which provide the first evidence for a deformation midway between normal and super deformed, can be interpreted in terms of the $[651] \frac{1}{2}$ and $[770] \frac{1}{2}$ neutron configurations.

PACS number(s): 21.10.Re, 21.10.Tg, 23.20.En, 27.70.+q

Three ellipsoidal shapes are commonly observed in stably deformed nuclei: prolate deformation with $\beta_2 \approx 0.25$ (normally deformed), super deformed prolate deformation with $\beta_2 \approx 0.55$, and oblate deformation with $\beta_2 \approx -0.15$. The increased stability of these shapes has been attributed to minima in the single-particle energies which can be related to highly ordered periodic single-particle orbits. In contrast, the occupation of certain highly polarizing, particlelike orbits will have a strong tendency to drive the nuclear shape away from these common deformations; see, e.g., [1]. Indeed, much of modern nuclear structure physics is concerned with the striking stability of these deformations, the single-particle dependence of the relatively small variations from these stable shapes, and what happens in less stably deformed "transitional" nuclei.

The present work reports the first evidence for a configuration in ^{186}Hg with a deformation midway between normal and super deformation. Calculations associate this configuration with the occupation of a pair of quasineutrons (either the $\nu([651] \frac{1}{2} \otimes [514] \frac{7}{2})$ or the $\nu([651] \frac{1}{2} \otimes [770] \frac{1}{2})$ configuration [2], or a mixture of these two) that intrude (at large deformations) from above the $N=126$ shell. The occupation of these orbitals also is expected for the super deformed configurations of the lighter osmium and platinum [3] and heavier mercury isotopes [4]. The interpretations of additional decay sequences, established in our work, will be presented later. Preliminary results have been reported previously [5].

Though the ground states of the mercury isotopes are known to be oblate, the shape-coexisting high-spin yrast states of the neutron-deficient mercury isotopes usually are thought to have a stable prolate deformation. Indeed, calculations based on different mean-field assumptions, see e.g. [6], all predict such a coexistence of oblate and prolate shapes. There was no prior experimental evi-

dence that establishes a negative parity for the intruder band (band 3 in Fig. 1) in ^{186}Hg . This band earlier was assigned positive parity and even spins and interpreted as an aligned $\nu(i_{13/2})^2$ configuration based on a triaxial core [7], or alternatively interpreted as an intruder $\pi(i_{13/2})^2$ configuration based on a prolate core [8]. In a recent study, band 3 was suggested [9] to have negative parity based on only one dipole DCD ratio (directional correlation orientated nuclei) (this does not distinguish $M1$ and $E1$), and discussed in terms of an aligned $\pi(i_{13/2} \otimes h_{9/2})$ configuration by analogy to the 11^- band in ^{184}Pt [10].

The ^{186}Hg nuclei were produced at the Holifield Heavy Ion Research Facility using the $^{154}\text{Gd}(^{36}\text{S}, 4n)$ reaction. Two ^{154}Gd targets (92% enriched) were used, a 1.0-mg/cm² self-supporting target and a 1.2-mg/cm² target backed by 6.2 mg/cm² of ^{197}Au . Gamma rays were detected with 20 Compton-suppressed Ge detectors in a compact geometry at a beam energy of 167 MeV, with excitation function data at 159 and 175 MeV. The self-supporting target yielded 2.7×10^8 , and the backed target 9.0×10^8 γ - γ events triggered by γ - γ - γ events. A four-Ge-detector Compton polarimeter was placed at 90°. A polarimeter event (2.3×10^7 collected) required a coincidence between two of the polarimeter detectors and at least one Compton-suppressed Ge detector.

A level scheme deduced from the present work is shown in Fig. 1. In most cases, spin and parity assignments are based on the measured DCO ratios. Band 2, interpreted as the lowest configuration in the prolate minimum, is extended to (28^+) . The DCO ratios of the 255- and 1011-keV transitions [0.60(5) and 0.69(6), respectively] indicate that both of them carry only one unit of angular momentum to yield a spin of 11 for the 3089-keV level. The linear polarization of the 255-keV γ ray, +0.40(28) (without efficiency correction), indicates that this transition is $E1$ ($M1$ transitions have negative values). Thus, band 3 starts from 11^- and is extended to (31^-) .

Doppler-broadened line shapes are established in the backed-target data, by comparing the spectra obtained

*Permanent address: Institute of Theoretical Physics, University of Warsaw, Warsaw, Poland.

from forward (45°) and backward (135°) angle detectors, at and above the 20⁺ → 18⁺ transition in band 2 and the 23⁻ → 21⁻ transition in band 3. Lifetimes were extracted by applying the Doppler shift attenuation method to spectra gated on transitions lying below the levels of interest. The line shapes at forward and backward angles were fitted simultaneously with a local version of the program DSAMFT [11], which includes a Monte Carlo simulation [12] of the nuclear stopping power. Tabulated electronic stopping powers corrected for shell effects [13] were used. A five-state rotational-band sidefeeding was assumed for each level. The transition quadrupole moments of the state under consideration (Q_t) and of the assumed sidefeeding cascade (Q_s) were extracted by minimizing the χ^2 of the fit.

As illustrated in Fig. 2, the measured line shapes are well reproduced. The contaminations were identified from forward and backward angle spectra. Their intensities were carefully controlled in the fitting process. Gamma-ray intensities and extracted quadrupole moments are summarized in Table I. A few details of the analysis are noteworthy. The transitions depopulating the 24⁺ and 27⁻ levels are the highest spin transitions fitted because of the limitation of statistics. The precursor

rotational transitions preceding these two levels were assumed to have similar Q_t values to their band members respectively. The errors related to this assumption, affecting especially the two top-most transitions, were evaluated by varying the precursor Q_t values $\pm 20\%$. The sidefeeding clearly can influence the state lifetimes. Current Q_s values of band 3 already are on average $\sim 30\%$ larger than those in band 2. It would require a significant further increase in these values to result in a Q_t of band 3 comparable to that of band 2. However, this is highly unlikely physically. The errors listed in Table I also include other statistical errors (counting statistics, uncertainties of the energy loss in the slowing-down process and correlated uncertainties from the fitting process). Finally, the sidefeeding intensities were changed by $\pm 20\%$ to add an additional error in the Q_t values.

The average Q_t values obtained for bands 2 and 3 are 7.7(1.3) and 10.7(1.7), respectively. Assuming axial symmetry, the standard formula $Q_t = 0.0109ZA^{2/3}\beta_2(1 + 0.36\beta_2)$ yields quadrupole deformations of $\beta_2 = 0.25(3)$ for band 2 and 0.34(4) for band 3. This value for band 2 agrees with the measured value for the lower spin members of this decay sequence [14] and other normally

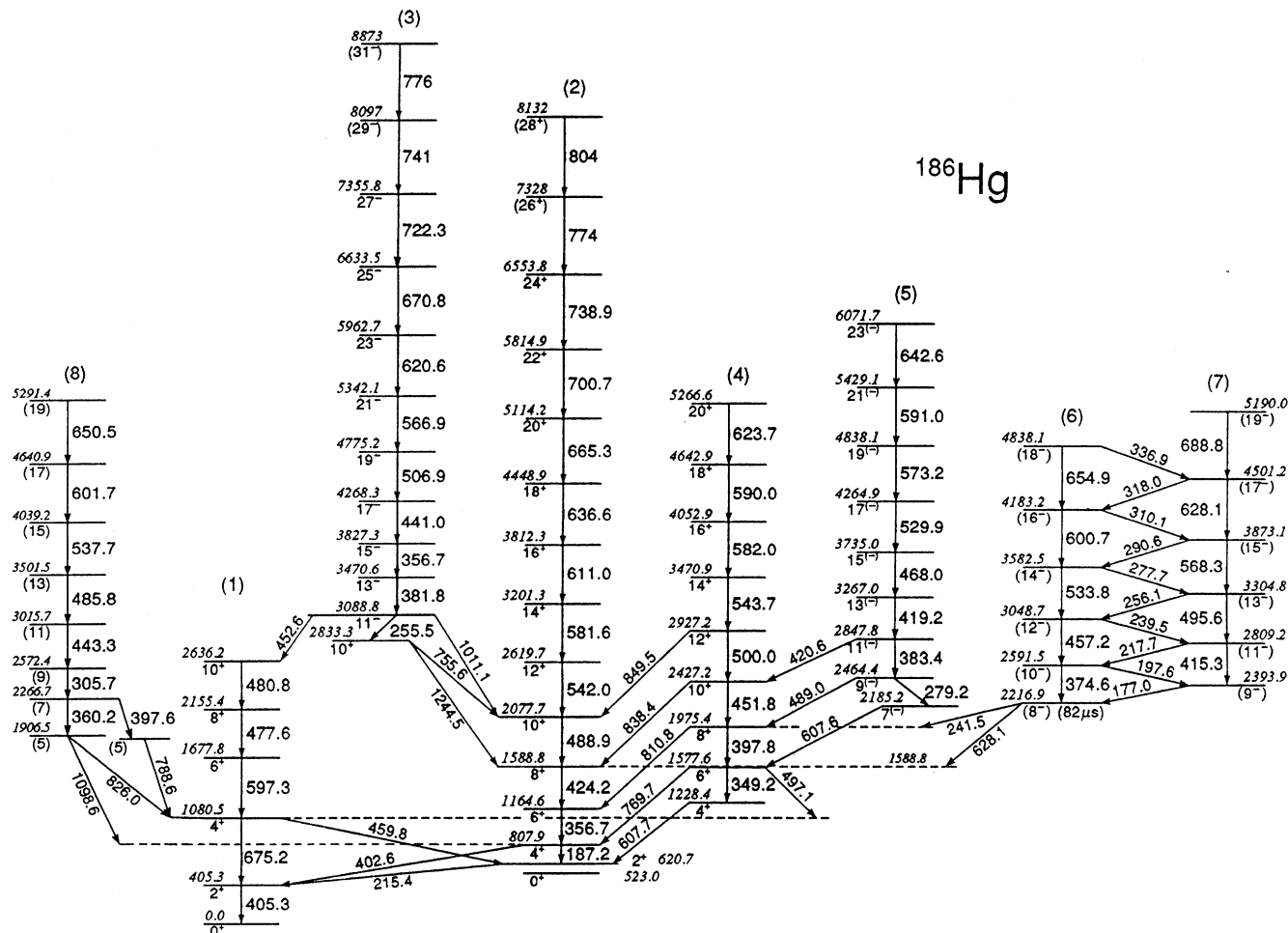


FIG. 1. ¹⁸⁶Hg level scheme from this study.

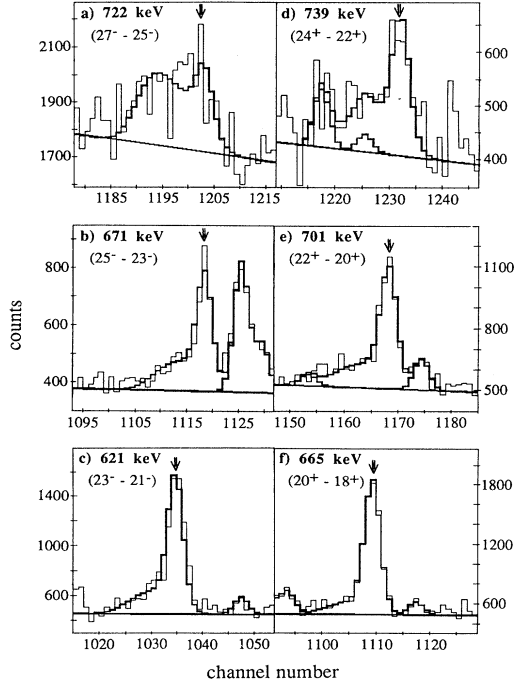


FIG. 2. Doppler-broadened line shapes seen by the backward angle detectors (thin line, experimental data; thick line, calculations which include the unshifted peak and moving components, also the contaminations). The arrows indicate the unshifted peak positions. See text for details.

deformed nuclei. A possible additional 15–20 % systematic error from uncertainties in the treatment of the slowing-down process does not alter the conclusion that the deformation of band 3 is significantly larger than that of band 2.

The previous interpretation of collective negative-parity intruder bands in this mass region involved $\pi(i_{13/2} \otimes h_{9/2})$ excitations based on a prolate core, e.g., in ^{184}Pt [10]. This same interpretation was given for band 3 in ^{186}Hg in Ref. [9]. However, we propose an alternative interpretation for this band. Woods-Saxon calculations [3] indicate that for $N=104-108$ the lowest, $1i_{11/2} \otimes 2g_{9/2}$ Nilsson neutron orbital ($[651]_{1/2}^-$) approaches the Fermi level at $\beta_2 \sim 0.35$. This state is the neutron analog of the $1h_{9/2} \otimes 2f_{7/2}$ ($[541]_{1/2}^+$) proton orbital. The inset in Fig. 3 shows the calculated band-head energies of the two low-lying $\pi = -$ two-quasiparticle $\pi([541]_{1/2}^- \otimes [660]_{1/2}^-)$ and $\nu([651]_{1/2}^- \otimes [514]_{7/2}^+)$ states in the mercury isotopes with $102 \leq N \leq 108$. The calculations were made using the Woods-Saxon-Strutinsky model with pairing

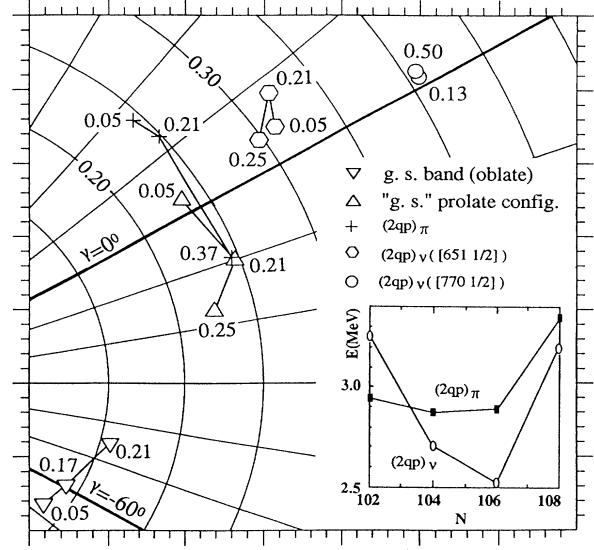


FIG. 3. Calculated equilibrium deformations of near-yrast configurations in ^{186}Hg in the β - γ polar coordinates. Predicted energies of the two-quasiparticle proton and neutron intruder states in $^{182-188}\text{Hg}$ are given in the inset. The rotational frequencies are indicated (in MeV/\hbar).

treated by the Lipkin-Nogami approach as described in Ref. [15]. In $^{184,186}\text{Hg}$ the $\nu([651]_{1/2}^- \otimes [514]_{7/2}^+)$ configuration is predicted 200 to 400 keV lower in energy than the two-quasiparticle proton configuration. In the Pt isotopes the pattern is similar, but both two-quasiparticle states lie about 3 MeV above the prolate ground state.

No rotational sequence based on the deformed $\nu[651]_{1/2}^-$ state has been established previously, and only a few possible candidates for this configuration are given in a recent systematic study of one-quasiparticle states in this mass region [16]. The $[651]_{1/2}^-$ state (strongly mixed with the $[640]_{1/2}^-$ state) is essential for producing strong octupole correlations in the light actinides through coupling with the $[770]_{1/2}^-$ orbital [17]. Likewise, the band crossing in superdeformed $^{146,147}\text{Gd}$ has been interpreted [18] in terms of the $\nu[651]_{1/2}^-$ orbital. Evidence for the presence of this neutron state at intermediate deformations would establish its deformation trajectory experimentally.

Aligned angular momenta for several bands in ^{186}Hg and that of the $\pi([541]_{1/2}^- \otimes [660]_{1/2}^-)$, negative-parity band in ^{184}Pt are shown in Fig. 4. The alignment pattern for band 3 is different from that of either band 2 or the band in ^{184}Pt . Whereas alignments attributed to a pair of $i_{13/2}$ neutrons occur at $\omega \sim 0.28$ MeV for both band 2 and the

TABLE I. Summary of γ -ray relative intensity and quadrupole moment information extracted from the lifetime measurements.

E_γ (keV)	$I_i^\pi \rightarrow I_f^\pi$	Intensity	Q_i (e b)	Q_s (e b)	χ^2
722.3	$27^- \rightarrow 25^-$	1.1(1)	$10.7(^{+3.7}_{-2.7})$	$7.6(^{-1.0}_{-3.5})$	2.06
670.8	$25^- \rightarrow 23^-$	2.0(2)	$11.2(^{-1.6}_{-1.6})$	$7.7(^{-2.0}_{+2.0})$	0.70
620.6	$23^- \rightarrow 21^-$	4.3(2)	$10.3(^{-2.4}_{-1.5})$	$10.8(^{-1.5}_{+2.0})$	0.96
738.9	$24^+ \rightarrow 22^+$	2.2(2)	$7.7(^{-2.5}_{-2.0})$	$5.2(^{-1.4}_{+1.3})$	0.54
700.7	$22^+ \rightarrow 20^+$	4.0(2)	$7.3(^{-1.3}_{-1.3})$	$6.7(^{-1.7}_{+1.7})$	0.59
665.3	$10^+ \rightarrow 18^+$	6.8(3)	$8.0(^{-1.3}_{-1.4})$	$5.6(^{-1.7}_{+3.7})$	0.75

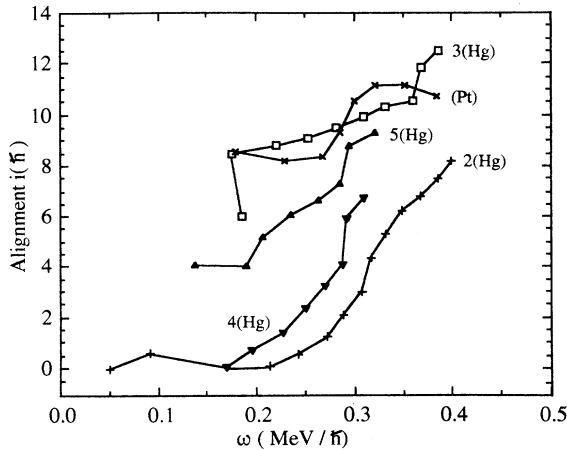


FIG. 4. Aligned angular momentum for bands in ^{186}Hg and the $\pi = -$ band in ^{184}Pt built on the 3081-keV state [9]. The reference parameters $J_0 = 30 \text{ } \hbar^2/\text{MeV}$, $J_1 = 110 \text{ } \hbar^4/\text{MeV}^2$ are used for both nuclei.

band in ^{184}Pt [10], this crossing is clearly absent in band 3, which looks very collective over the total range of observed frequencies.

Figure 3 also displays calculated equilibrium deformations extracted from the total Routhian surfaces for near-yrast configurations in ^{186}Hg , corresponding to different ω values near the $\nu i_{13/2}$ band crossing. The relationship between Q_t and β_2 from Ref. [19] was used to account for β_4 , γ and higher-order terms of β_2 . Shape-coexisting bands built on the oblate (ground state, $\beta_2 \sim 0.15$, $\gamma \sim -60^\circ$) and prolate ($\beta_2 \sim 0.23$, $\gamma \sim 0^\circ$) 0^+ states are indicated by the triangles. The alignment of $i_{13/2}$ neutrons triggers a shape change towards $\gamma \sim -15^\circ$ for the prolate band. The calculated Q_t value for band 2 is 9.1 e b, somewhat larger than the experimental value. The deformation of the $\pi([541]_{1/2}^+ \otimes [660]_{1/2}^-)$ band is predicted to be $\beta_2 \sim 0.25$, i.e., nearly equal to that of the pro-

late yrast band, but with a slightly positive value of $\gamma \sim 10^\circ$. The calculated equilibrium deformation of the $\nu([651]_{1/2}^+ \otimes [514]_{7/2}^-)$ configuration is about $\beta_2 \sim 0.31$ ($Q_t \approx 11.1 \text{ e b}$), i.e., it is intermediate between the deformation for the prolate minimum ($\beta_2 \sim 0.23$) and the deformation of superdeformed states in the heavier Hg isotopes ($\beta_2 \sim 0.48$) [4]. Finally, the equilibrium deformations of the intruder band involving the lowest $N = 7$ neutron, i.e., the $\nu([651]_{1/2}^+ \otimes [770]_{1/2}^-)$ band is predicted to be $\beta_2 \sim 0.41$ ($Q_t \approx 15.8 \text{ e b}$).

The experimental quadrupole moment $Q_t = 10.7(1.7)$ for band 3 may be consistent with either interpretation, since the experimental values are systematically smaller than the calculated ones. Another attractive possibility, which is difficult to confirm by experiment, involves octupole mixing between the $j_{15/2}$ and $i_{11/2} \oplus g_{9/2}$ neutron states (as mentioned earlier this mixing plays a crucial role in producing static octupole deformations in the light actinides).

In summary, evidence is presented for a negative-parity, odd-spin decay sequence in ^{186}Hg which has a quadrupole moment that is about 40% larger than that of the normally deformed yrast sequence. This band, the first in heavy deformed nuclei with an established deformation midway between normal and super deformed, is interpreted as an excitation of two highly deformation-polarizing quasineutrons, either the $\nu([651]_{1/2}^+ \otimes [514]_{7/2}^-)$ or the $\nu([651]_{1/2}^+ \otimes [770]_{1/2}^-)$ configuration or a combination of both intruding from above the $N = 126$ shell.

This work was supported by the U.S. DOE under Grant DE-FG05-88ER40407 with Vanderbilt and Grant DE-AC05-84OR21400 with Martin Marietta Energy Systems, Inc. The Joint Institute for Heavy Ion Research is supported by its members, the University of Tennessee, Vanderbilt University, and Oak Ridge National Laboratory and by DOE Contract DE-FG05-87ER40361 with the University of Tennessee.

- [1] W. Nazarewicz, in *Contemporary Topics in Nuclear Structure Physics*, edited by R. F. Casten *et al.* (World-Scientific, Singapore, 1988), p. 467.
- [2] The configurations are indicated by means of spherical labels, proper for unique-parity orbitals and normal deformations or, alternatively, by asymptotic labels, more appropriate at large deformations.
- [3] R. Wyss, W. Satula, W. Nazarewicz, and A. Johnson, *Nucl. Phys.* **A511**, 324 (1990).
- [4] R. V. F. Janssens and T. L. Khoo, *Annu. Rev. Nucl. Part. Sci.* **41**, 321 (1991).
- [5] W. C. Ma *et al.*, Vanderbilt Annual Reports DOE/ER/40407-03, 1990 and DOE/ER/40407-04, 1991; J. H. Hamilton, in *International Conference on Nuclear Shapes and Nuclear Structure at Low Excitation Energies*, edited by M. Vergnes *et al.* (Cargese, France, 1991) (Plenum, New York, 1992), p. 17.
- [6] S. Aberg, H. Flocard, and W. Nazarewicz, *Annu. Rev. Nucl. Part. Sci.* **40**, 439 (1990).
- [7] R. V. F. Janssens *et al.*, *Phys. Lett.* **131B**, 35 (1983).
- [8] W. C. Ma *et al.*, *Phys. Lett.* **167B**, 277 (1986).
- [9] M. G. Porquet, G. Bastin, C. Bourgeois, A. Korichi, N. Perrin, H. Sergolle, and F. A. Beck, *J. Phys. G* **18**, L29 (1992).
- [10] M. P. Carpenter *et al.*, *Nucl. Phys.* **A513**, 125 (1990).
- [11] J. Gascon *et al.*, *Nucl. Phys.* **A513**, 744 (1990).
- [12] J. C. Bacelar, R. M. Diamond, E. M. Beck, M. A. Deleplanque, J. Draper, and F. S. Stephens, *Phys. Rev. C* **35**, 1170 (1987).
- [13] L. C. Northcliffe and R. F. Schilling, *Nucl. Data Tables* **7**, 233 (1970); J. F. Ziegler and W. K. Chu, *At. Data Nucl. Data Tables* **13**, 463 (1974); D. Ward, J. S. Foster, H. R. Andrews, I. V. Mitchell, G. C. Ball, W. G. Davies, and G. J. Gosta, *At. En. Canada Ltd. Report AECL-5313*, 1976.
- [14] D. Proetel, R. M. Diamond, and F. S. Stephens, *Phys. Lett.* **48B**, 102 (1976).
- [15] W. Nazarewicz, M. A. Riley, and J. D. Garrett, *Nucl. Phys.* **A512**, 61 (1990).
- [16] A. K. Jain, R. S. Sheline, R. C. Sood, and K. Jain, *Rev. Mod. Phys.* **62**, 392 (1990).
- [17] G. A. Leander and Y. S. Chen, *Phys. Rev. C* **37**, 2744 (1988).
- [18] G. Hebbinghaus *et al.*, *Phys. Lett. B* **240**, 311 (1990).
- [19] W. Nazarewicz, R. Wyss, and A. Johnson, *Nucl. Phys.* **A503**, 285 (1989).